

Escherlike quasiperiodic heterostructures

Alberto G. Barriuso,¹ Juan J. Monzón,¹ Luis L. Sánchez-Soto,¹ and Antonio F. Costa²

¹*Departamento de Óptica, Facultad de Física, Universidad Complutense, 28040 Madrid, Spain*

²*Departamento de Matemáticas Fundamentales, Facultad de Ciencias,*

Universidad Nacional de Educación a Distancia, Senda del Rey 9, 28040 Madrid, Spain

(Dated: February 2, 2022)

We propose quasiperiodic heterostructures associated with the tessellations of the unit disk by regular hyperbolic triangles. We present explicit construction rules and explore some of the properties exhibited by these geometric-based systems.

PACS numbers: 61.44.Br, 68.65.Cd, 71.55.Jv, 78.67.Pt

Quasiperiodic (QP) systems have been receiving a lot of attention over the last years [1]. The interest was originally motivated by the theoretical predictions that they should manifest peculiar electron and phonon critical states [2, 3], associated with highly fragmented fractal energy spectra [4, 5, 6]. On the other hand, the practical fabrication of Fibonacci [7] and Thue-Morse [8] superlattices has triggered a number of experimental achievements that have provided new insights into the capabilities of QP structures [9]. In particular, possible optical applications have deserved major attention and some intriguing properties have been demonstrated [10, 11, 12, 13]. Underlying all these theoretical and experimental efforts a crucial fundamental question remains concerning whether QP devices would achieve better performance than usual periodic ones for some specific applications [14].

The QP systems considered thus far rely for their explicit construction in substitutional rules among the elements of a basic alphabet. In the common case of a two-letter alphabet $\{A, B\}$, the algorithm takes the form $A \mapsto \sigma_A(A, B)$, $B \mapsto \sigma_B(A, B)$, where σ_A and σ_B can be any string of the letters. The sequences generated after n applications of the algorithm are of significance in fields as diverse as cryptography, time-series analysis, and cellular automata [15]. In addition, they have interesting algebraic properties, which are usually characterized by the nature of their Fourier or multifractal spectra [16].

We wish to approach the problem from an alternative geometrical perspective. To this end, we first observe that in many problems of physical interest [17] the letters of the alphabet can be identified with one-dimensional linear lossless systems (i.e., with two input and two output channels). Under these general conditions, it turns out that the associated transfer matrix belongs to the group $SU(1,1)$, which is also the basic symmetry group of the hyperbolic geometry [18]. In consequence, the unit disk appears as the natural arena to discuss their performance [19, 20, 21]. Since in the Euclidean plane, QP behavior is intimately linked with tessellations, one is unfailingly led to consider the role of hyperbolic tessellations in the unit disk, much in the spirit of Escher's masterpiece woodcut *Circle Limit III* [22]. The answer we propose is promising: the tessellations by different regular polygons provide new sequences with properties that may open avenues

of research in this field.

A QP system can thus be seen as a word generated by stacking different letters of the basic alphabet. To be specific, we focus our attention on the optical response. Let us consider one of these letters (which in practice is made of several plane-parallel layers), which we assume to be sandwiched between two semi-infinite identical ambient (a) and substrate (s). We suppose monochromatic plane waves incident, in general, from both the ambient and the substrate. As a result of multiple reflections in all the interfaces, the total electric field can be decomposed in terms of forward- and backward-traveling plane waves, denoted by $E^{(+)}$ and $E^{(-)}$, respectively. If we take these components as a vector

$$\mathbf{E} = \begin{pmatrix} E^{(+)} \\ E^{(-)} \end{pmatrix}, \quad (1)$$

then the amplitudes at both the ambient and the substrate sides are related by the transfer matrix \mathbf{M}

$$\mathbf{E}_a = \mathbf{M} \mathbf{E}_s. \quad (2)$$

It can be shown that \mathbf{M} is of the form

$$\mathbf{M} = \begin{pmatrix} 1/T & R^*/T^* \\ R/T & 1/T^* \end{pmatrix}, \quad (3)$$

where the complex numbers R and T are, respectively, the overall reflection and transmission coefficients for a wave incident from the ambient. The condition $\det \mathbf{M} = +1$ is equivalent to $|R|^2 + |T|^2 = 1$, and then the set of transfer matrices reduces to the group $SU(1,1)$. Obviously, the matrix of a word obtained by putting together letters of the alphabet is the product of the matrices representing each one of them, taken in the appropriate order.

In many instances we are interested in the transformation properties of field quotients rather than the fields themselves. Therefore, it seems natural to consider the complex numbers

$$z = \frac{E^{(-)}}{E^{(+)}} \quad (4)$$

for both ambient and substrate. The action of the matrix given in Eq. (2) can be then seen as a function $z_a = f(z_s)$ that can be appropriately called the transfer function. From a geometrical viewpoint, this function defines a transformation of the

complex plane \mathbb{C} , mapping the point z_s into the point z_a according to

$$z_a = \frac{\beta^* + \alpha^* z_s}{\alpha + \beta z_s}, \quad (5)$$

where $\alpha = 1/T$ and $\beta = R^*/T^*$. When no light is incident from the substrate, $z_s = 0$ and then $z_a = R$. Equation (5) is a bilinear (or Möbius) transformation. One can check that the unit disk, the external region and the unit circle remain invariant under (5). This unit disk is then a model for hyperbolic geometry in which a line is represented as an arc of a circle that meets the boundary of the disk at right angles to it (and diameters are also permitted). In this model, we have three different kinds of lines: intersecting, parallel (they intersect at infinity, which is precisely the boundary of the disk) and ultraparallel (they are neither intersecting nor parallel).

To classify the possible actions it proves convenient to work out the fixed points of the transfer function; that is, the field configurations such that $z_a = z_s \equiv z_f$ in Eq. (5), whose solutions are

$$z_f = \frac{1}{2\beta} \left\{ -2i \operatorname{Im}(\alpha) \pm \sqrt{[\operatorname{Tr}(\mathbf{M})]^2 - 4} \right\}. \quad (6)$$

When $[\operatorname{Tr}(\mathbf{M})]^2 < 4$ the action is elliptic and it has only one fixed point inside the unit disk. Since in the Euclidean geometry a rotation is characterized for having only one invariant point, this action can be appropriately called a hyperbolic rotation.

When $[\operatorname{Tr}(\mathbf{M})]^2 > 4$ the action is hyperbolic and it has two fixed points, both on the boundary of the unit disk. The geodesic line joining these two fixed points remains invariant and thus, by analogy with the Euclidean case, this action is called a hyperbolic translation.

Finally, when $[\operatorname{Tr}(\mathbf{M})]^2 = 4$ the action is parabolic and it has only one (double) fixed point on the boundary of the unit disk.

As it is well known, $SU(1, 1)$ is isomorphic to the group of real unimodular matrices $SL(2, \mathbb{R})$, which allows us to translate the geometrical structure defined in the unit disk to the complex upper semiplane, recovering in this way an alternative model of the hyperbolic geometry that is useful in some applications.

The notion of periodicity is intimately connected with tessellations, i.e., tilings by identical replicas of a unit cell (or fundamental domain) that fill the plane with no overlaps and no gaps. Of special interest is the case when the primitive cell is a regular polygon with a finite area [23]. In the Euclidean plane, the associated regular tessellation is generically noted $\{p, q\}$, where p is the number of polygon edges and q is the number of polygons that meet at a vertex. We recall that geometrical constraints limit the possible regular tilings $\{p, q\}$ to those verifying $(p-2)(q-2) = 4$. This includes the classical tilings $\{4, 4\}$ (tiling by squares) and $\{6, 3\}$ (tiling by hexagons), plus a third one, the tiling $\{3, 6\}$ by triangles (which is dual to the $\{6, 3\}$).

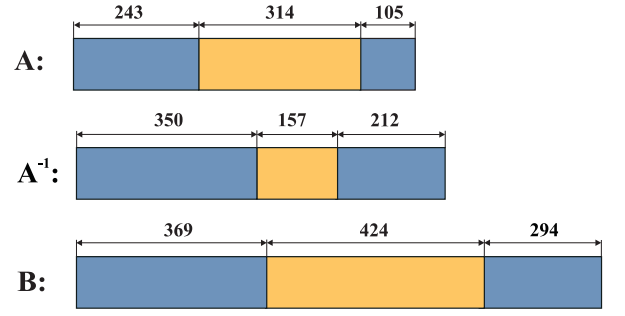


FIG. 1: (color online). A realistic implementation of the generators **A** and **B** (together with \mathbf{A}^{-1}) of the tessellations by hyperbolic triangles in (7). The external layers (in blue) are made of cryolite (Na_3AlF_6), while the central medium (in brown) is zinc selenide (ZnSe). The wavelength in vacuum is $\lambda = 610$ nm and normal incidence (from left to right) has been assumed. The corresponding thicknesses are expressed in nanometers.

On the contrary, in the hyperbolic disk regular tilings exist provided $(p-2)(q-2) > 4$, which now leads to an infinite number of possibilities. An essential ingredient is the way to obtain fundamental polygons. These polygons are directly connected to the discrete subgroups of isometries (or congruent mappings). Such groups are called Fuchsian groups [24] and play for the hyperbolic geometry a role similar to that of crystallographic groups for the Euclidean geometry [25].

A tessellation of the hyperbolic plane by regular polygons has a symmetry group that is generated by reflections in geodesics, which are inversions across circles in the unit disk. These geodesics correspond to edges or axes of symmetry of the polygons. Therefore, to construct a tessellation of the unit disk one just has to build one tile and to duplicate it by using reflections in the edges.

In this Letter, we consider only the simple example of a tessellation by triangles with vertices in the unit circle, although the treatment can be extended to other polygons. The key idea is to consider the Fuchsian group generated by an elliptic transformation whose fixed point is the middle of an edge of the triangle and a parabolic one with its fixed point in the opposite vertex. Proceeding in this way we get

$$\begin{aligned} \mathbf{A} &= \begin{pmatrix} 1 + i/\sqrt{3} & 1/\sqrt{3} \\ 1/\sqrt{3} & 1 - i/\sqrt{3} \end{pmatrix}, \\ \mathbf{B} &= \begin{pmatrix} 2i/\sqrt{3} & -1/\sqrt{3} \\ -1/\sqrt{3} & -2i/\sqrt{3} \end{pmatrix}. \end{aligned} \quad (7)$$

The fixed point of **A** is $-i$; while for **B** the fixed point in the disk is $i(2 - \sqrt{3})$. In Fig. 1 we show a possible way in which these matrices can be implemented in terms of two commonly employed materials in optics. Note that, in physical terms, the inverses must be constructed as independent systems, although in our case only \mathbf{A}^{-1} must be considered, since the action of \mathbf{B}^{-1} coincides with that of **B**.

In Fig. 2 we have shown the tessellation obtained by transforming the fundamental triangle with the Fuchsian group

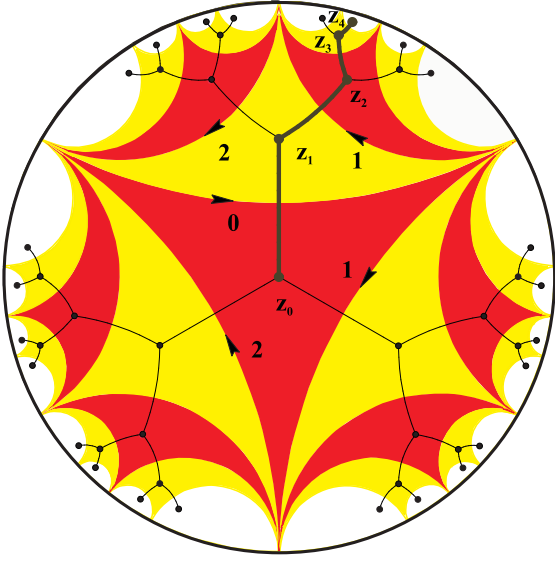


FIG. 2: (color online). Tiling of the unit disk with the matrices (7). The marked points are the barycenters of the triangles in the tessellation and all of them are the transformed of the origin by a matrix that have as reflection coefficient the complex number that links the origin with the center of the triangle.

generated by the powers of $\{\mathbf{A}, \mathbf{B}\}$ (and the inverses). This triangle is equilateral with vertices at the points $-i$, $\exp(i\pi/6)$ and $\exp(i5\pi/6)$ (which are the fixed points of \mathbf{A} , \mathbf{AB} and \mathbf{BA} , respectively). Moreover, all the other triangles are equal, with an area π . In the figure we have plotted also the barycenters of each triangle together with the resulting tree (that is called the dual graph of the tessellation), which turns out to be a Farey tree [26]. In fact, each line connecting two of these barycenters represent the action of a word (with alphabet $\{\mathbf{A}, \mathbf{B}\}$ and the inverses).

To give an explicit construction rule for the possible words, we proceed as follows. First, we arbitrarily assign the number 0 to the upper side of the fundamental triangle, while the other two sides are clockwise numbered as 1 and 2. It is easy to convince oneself that this assignment fixes once for all the numbering for the sides of the other triangles in the tessellation. However, these triangles can be distinguished by their orientation (as seen from the corresponding barycenter): the clockwise oriented are filled in red, while the counterclock-

TABLE I: Explicit rules to obtain the barycenter z_{n+1} from the z_n . We have indicated the corresponding transformations, which depend on the color jumps and the sides crossed by going from z_n to z_{n+1} .

red \rightarrow yellow				yellow \rightarrow red			
Side	Trans	\mathbf{A}_{n+1}	\mathbf{B}_{n+1}	Trans	\mathbf{A}_{n+1}	\mathbf{B}_{n+1}	
0	\mathbf{B}_n	$\mathbf{B}_n \mathbf{A}_n \mathbf{B}_n$	\mathbf{B}_n	\mathbf{B}_n	$\mathbf{B}_n \mathbf{A}_n^{-1} \mathbf{B}_n$	\mathbf{B}_n	
1	\mathbf{A}_n	\mathbf{A}_n	$\mathbf{A}_n \mathbf{B}_n \mathbf{A}_n^{-1}$	\mathbf{A}_n^{-1}	\mathbf{A}_n	$\mathbf{A}_n^{-1} \mathbf{B}_n \mathbf{A}_n$	
2	\mathbf{A}_n^{-1}	\mathbf{A}_n^{-1}	$\mathbf{A}_n^{-1} \mathbf{B}_n \mathbf{A}_n$	\mathbf{A}_n	\mathbf{A}_n^{-1}	$\mathbf{A}_n \mathbf{B}_n \mathbf{A}_n^{-1}$	

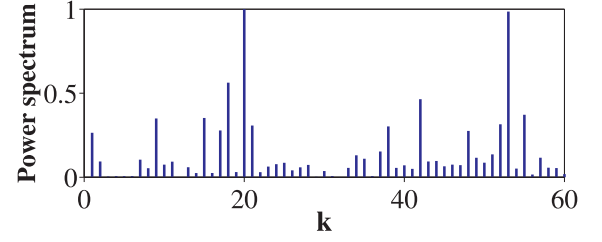


FIG. 3: (color online). Normalized structure factor for the word (made of 60 letters) connecting the origin with the point z_8 in the zig-zag path shown in Fig. 2.

wise are filled in yellow. In short, we have determined a fundamental coloring of the tessellation [27].

To obtain one barycenter z_{n+1} from the previous one z_n , one looks first at the corresponding color jump. Next, the matrix that take z_n into z_{n+1} depends on the numbering of the side (0, 1, or 2) one must cross, and appear in the appropriate column “Trans” in Table I. The next generation is obtained much in the same way, except for the fact that \mathbf{A}_n and \mathbf{B}_n must be replaced by \mathbf{A}_{n+1} and \mathbf{B}_{n+1} , respectively, as indicated in the Table. In obtaining recursively any word, the origin is denoted as z_0 and the matrices \mathbf{A}_0 and \mathbf{B}_0 coincide with \mathbf{A} and \mathbf{B} .

With this rule, one can construct any word proceeding step by step. For example, the word that transform z_0 into z_5 in the zig-zag path sketched in Fig. 2 results

$$\begin{aligned}
 z_0 \rightarrow z_1 &: \mathbf{B}, \\
 z_1 \rightarrow z_2 &: \mathbf{BA}^{-1}\mathbf{B}, \\
 z_2 \rightarrow z_3 &: \mathbf{BA}^{-1}\mathbf{B}, \\
 z_3 \rightarrow z_4 &: \mathbf{BA}^{-1}\mathbf{A}^{-1}\mathbf{BAAB}, \\
 z_4 \rightarrow z_5 &: \mathbf{BA}^{-1}\mathbf{A}^{-1}\mathbf{BABAAB}.
 \end{aligned} \tag{8}$$

Obviously, the total word is obtained by composing these partial words.

In fact, one can show that given an arbitrary sequence of nonzero integers $\{k_1, k_2, \dots, k_r\}$, the word represented by the transfer matrix

$$\mathbf{M}(s, k_1, \dots, k_r) = \mathbf{B}^{s_1} \mathbf{A}^{k_1} \mathbf{BA}^{k_2} \dots \mathbf{BA}^{k_r} \mathbf{B}^{s_2}, \tag{9}$$

where $\{s_1, s_2\} \subset \{0, 1\}$, transforms the origin in a barycenter of the tessellation.

Given the geometric regularity of the construction sketched in this Letter, the sequences obtained must play a key role in the theory and practice of QP systems. Of course, to put forward the relevant physical features of these sequences, there are a number of quantities one can look at. Perhaps one of the most appropriate ones to assess the performance of these systems is the structure factor [15]. For a word \mathbf{M} (composed of L letters) we define a numerical sequence f_n by assigning 1, $e^{2\pi i/3}$, and $e^{-2\pi i/3}$ to the letters \mathbf{B} , \mathbf{A} , and \mathbf{A}^{-1} , respectively. Next, we calculate the discrete Fourier transform of the

sequence f_n

$$F_k = \sum_{n=0}^{L-1} f_n \exp\left(-\frac{2\pi i k n}{L}\right), \quad (10)$$

where $k = 0, 1, \dots, L-1$. The structure factor (or power spectrum) is just $|F_k|^2$. In Fig. 3 we have plotted this structure factor in terms of k for the word connecting the origin with the point z_8 in the zig-zag path of Fig. 2. The peaks reveal a rich behavior: a full analysis of these questions is outside the scope of this Letter and will be presented elsewhere.

As a final and rather technical remark, we note that the quotient of the hyperbolic disk by the Fuchsian group generated by **A** and **B** is a 2-orbifold of genus 0, with a conical point of order two and a cusp. Each word as given in Eq. (9) represents a hyperbolic transformation of the disk, and the axis of the transformation is projected onto a closed geodesic of such an orbifold. This provides an orbifold interpretation of our QP sequences.

In summary, we expect to have presented new schemes to generate QP sequences based on hyperbolic tessellations of the unit disk. Apart from the intrinsic beauty of the formalism, our preliminary results seem to be quite encouraging for future applications of these systems.

The authors wish to express their warmest gratitude to E. Maciá and J. M. Montesinos for their help and interest in the present work.

-
- [1] E. Maciá, Rep. Prog. Phys. **69**, 397 (2006).
 - [2] S. Ostlund and R. Pandit, Phys. Rev. B **29**, 1394 (1984).
 - [3] M. Kohmoto, B. Sutherland, and K. Iguchi, Phys. Rev. Lett. **58**, 2436 (1987).
 - [4] M. Kohmoto, L. P. Kadanoff, and C. Tang, Phys. Rev. Lett. **50**, 1870 (1983).
 - [5] A. Sütö, J. Stat. Phys. **56**, 525 (1989).

- [6] J. Bellissard, B. Iochum, E. Scoppola, and D. Testard, Comm. Math. Phys. **125**, 527 (1989).
- [7] R. Merlin, K. Bajema, R. Clarke, F. Y. Juang, and P. K. Bhat-tacharya, Phys. Rev. Lett. **55**, 1768 (1985).
- [8] R. Merlin, K. Bajema, J. Nagle, and K. Ploog, J. Phys. Colloq. **48**, C5 503 (1987).
- [9] V. R. Velasco and F. García-Moliner, Prog. Surf. Sci. **74**, 343 (2003).
- [10] S. Tamura and F. Nori, Phys. Rev. B **40**, 9790 (1989).
- [11] M. S. Vasconcelos and E. L. Albuquerque, Phys. Rev. B **59**, 11128 (1999).
- [12] D. Lusk, I. Abdulhalim, and F. Placido, Opt. Commun. **198**, 273 (2001).
- [13] A. G. Barriuso, J. J. Monzón, L. L. Sánchez-Soto, and A. Felipe, Opt. Express **13**, 3913 (2005).
- [14] E. Maciá, Phys. Rev. B **63**, 205421 (2001).
- [15] Z. Cheng and R. Savit, J. Stat. Phys. **60**, 383 (1990).
- [16] V. W. Spinadel, Nonlinear Anal. **36**, 721 (1999).
- [17] E. Maciá and R. Rodríguez-Oliveros, Phys. Rev. B **74**, 144202 (2006).
- [18] H. S. M. Coxeter, *Non-Euclidean Geometry* (University of Toronto Press, Toronto, 1968).
- [19] T. Yonte, J. J. Monzón, L. L. Sánchez-Soto, J. F. Cariñena, and C. López-Lacasta, J. Opt. Soc. Am. A **19**, 603 (2002).
- [20] J. J. Monzón, T. Yonte, L. L. Sánchez-Soto, and J. F. Cariñena, J. Opt. Soc. Am. A **19**, 985 (2002).
- [21] A. G. Barriuso, J. J. Monzón, and L. L. Sánchez-Soto, Opt. Lett. **28**, 1501 (2003).
- [22] H. S. M. Coxeter, Math. Intell. **18**, 42 (1996).
- [23] H. Zieschang, E. Vogt, and H. D. Coldeway, *Surfaces and planar discontinuous groups*, vol. 835 of *Lect. Not. Math.* (Springer, Berlin, 1980).
- [24] L. R. Ford, *Automorphic functions* (Chelsea Publishing Company, New York, 1972).
- [25] A. F. Beardon, *The geometry of discrete groups* (Springer, Berlin, 1983).
- [26] M. R. Schröder, *Number Theory in Science and Communication* (Springer, New York, 2006), 4th ed.
- [27] B. Grünbaum and G. C. Shepard, *Tilings and Patterns* (Freeman, New York, 1987).